Spin-flip transitions caused by ^{6}Li inelastic scattering and a microscopic α-spectator model*

K.-I. Kubo,† K. Nagatani, and K. G. Nair
Cyclotron Institute, Texas A&M University, College Station, Texas 77843
(Received 27 September 1976)

Inelastic deuteron scattering on ^{12}C has been studied using a microscopic description for both target and projectile nuclei. From the fits of the calculated results to the experimental data, the effective two-body interaction strength has been extracted. The Wigner part of the interaction was obtained from the analysis of the 4.43-MeV (2^+) state excitation and the result is compared with those found previously. The spin-spin part of the interaction was examined by the analysis of the 12.71-MeV (1^+) state. In addition, the consistency of our results was also checked by analyzing inelastic ^{3}He scattering. The real purpose of the present work was, however, to investigate such a treatment when applied to heavier projectile scattering. For this purpose, the inelastic ^{6}Li scattering leading to the 12.71-MeV (1^+) state was studied. Assuming the transition to be a spin-flip process, an α-spectator model based on the cluster description of ^{6}Li was used. Therefore, this analysis may be considered an extension of the ordinary microscopic treatment with the nucleon-nucleon interaction to the cluster description. The results of the effective interaction strengths are presented for various radial shapes of the nucleon-nucleon interaction. The effects of more complicated possible processes are also discussed.

[NUCLEAR REACTIONS Microscopic calculations of differential cross sections: ^{12}C(d,d'), $E=28$, 52 MeV; ^{12}C(^{3}He,^{3}He'), $E=49.8$ MeV; ^{12}C(^{6}Li,^{6}Li'), $E=36.4$ MeV; α-spectator model for (^{6}Li,^{6}Li'); deduced effective two-body interaction strengths.]

I. INTRODUCTION

Nuclear inelastic scattering processes have been studied in various contexts. Analyses are usually made using the distorted wave Born approximation (DWBA). Macroscopic form factors are commonly adopted in such calculations, since the procedure is very simple and generally provides good fits to experimental results. However, the model is almost completely phenomenological. In order to make a more fundamental approach, the form factor must be calculated in a microscopic treatment. For light-ion projectiles, such a formalism has been presented by Madsen,[1] where the individual nucleons in the projectile and target nuclei are explicitly described by their wave functions and the nucleon-nucleon interaction between them is folded in.

However, an extension of the treatment to heavy-ion scattering will result in very complicated computations since the number of nucleons (thus the number of degrees of freedom) is vastly increased. The familiar folding potential model provides a method of simplification, since the individual nucleons involved are described by the average nucleon density function. In fact, a recent analysis[2] of several cases of heavy-ion inelastic scattering based on such a model has been reasonably successful. However, a limitation of this model consists in replacing the nuclear wave functions by the derivative of average density functions so that the explicit behavior of the nucleons is never traced in the process.

The present study was carried out to explore the standard microscopic treatment of the form factor in the DWBA analysis for heavy-ion inelastic processes. The basic concept is an adaptation of a cluster-model description for the projectile nucleus. The form factor is evaluated by summing the cluster-nucleon interaction just as the ordinary microscopic calculation does with the nucleon-nucleon interaction. It is obvious that this procedure restricts the number of degrees of freedom to be small resulting in simplified calculations. Such a treatment has been applied[3] to the transfer reaction ^{12}C(^{7}Li,^{6}Li)^{13}C(g.s.). The ^{7}Li and ^{6}Li nuclei were described in terms of the $(\alpha+t)$ and $(\alpha+d)$ cluster structures, respectively. Then the reaction could be interpreted as a quasi-(t,d) reaction and it was found that this model reproduces the observed data very well.

In the present study, a very specific process, i.e., the inelastic transition ^{12}C(0^+) → ^{12}C 12.71 MeV ($1^+, T=0$) induced by the (d,d') and (^{6}Li,^{6}Li') reactions is considered because of the following reasons.[4] The residual 1^+ state is well described by the simple one-particle–one-hole configuration, $(p_{3/2}^{-1}p_{1/2})$. Thus the transition corresponds to a spin-flip process which may be caused by the spin-spin part [the $(\vec{\sigma}\cdot\vec{\sigma})$ type] in the nucleon-nucleon interaction. The (d,d') process is studied in terms of the ordinary microscopic formalism.[1] A cluster

description is applied to the (^{6}Li,^{6}Li′) process, since the ^{6}Li nucleus can be well expressed by the $(\alpha+d)$ configuration. Then the spin-flip transition is caused only by the interaction between the d cluster and the nucleon in ^{12}C. Since the α cluster does not contribute to this particular transition in the first order, we may refer to this excitation model as the "α-spectator" model.

To pursue the actual analysis, the effective interaction between the d cluster and the valence nucleon in ^{12}C is needed. We obtain such an interaction from the microscopic calculation of the same spin-flip transition in ^{12}C by the (d,d') process. The result of this calculation is compared and fitted to the experimental data[5,6] at 28 MeV, the only data available for this reaction, to the best of our knowledge. However, the incident energy is rather low and the consequent momentum mismatch problem might result in some ambiguity concerning the effective interaction extracted in the framework of DWBA. Therefore the consistency is also tested by comparing the $(\vec{\sigma}\cdot\vec{\sigma})$ type nucleon-nucleon interaction from the study of the ^{12}C(^{3}He,^{3}He′)^{12}C 12.71 MeV (1^+) reaction at 49.8 MeV.[7] The (d,d') excitation form factor thus obtained is utilized in the (^{6}Li,^{6}Li′) process. A comparison to the data is then expected to provide a test for the validity of the α-spectator model.

It should be straightforward to compare such an effective $(\vec{\sigma}\cdot\vec{\sigma})$ type interaction obtained from the analyses of the composite projectile scattering data with those obtained from the (p,p') analyses. However, the (p,p') processes leading to the ^{12}C 12.71-MeV ($1^+, T=0$) state as well as 15.11-MeV ($1^+, T=1$) state at low incident energies are rather complicated[8,9] and important contributions from exchange processes,[10] and tensor forces[11] have been pointed out. It is, therefore, one of the present motivations to analyze the (d,d') data, in order to know whether they can be simply interpreted by the ordinary $(\vec{\sigma}\cdot\vec{\sigma})$ type central interaction.

In order to make the analyses complete, the transition to the ^{12}C 4.43-MeV (2^+) state from the (d,d') reaction at 28 MeV is also studied in terms of the microscopic description. The nucleon-nucleon interaction extracted from this analysis is compared with those obtained by Hinterberger *et al.*[12] from the (d,d') process at 52 MeV, and by Ball and Cerny[7] from the (^{3}He,^{3}He′) process at 49.8 MeV.

The DWBA formalism for the α-spectator model is given in Sec. II. Physical parameters used in the following numerical calculations are described and summarized in Sec. III. The results of calculations are dealt with in Sec. IV. General discussions and concluding remarks are given in Secs. V and VI, respectively.

II. DISTORTED WAVE FORMALISM

The microscopic description of nuclear inelastic excitations induced by composite projectiles has been formulated by Madsen.[1] He has given general expressions of the nuclear transition matrix element and the differential cross section for the inelastic scattering of projectiles from $A=2$ to 4. The spin-orbit distortion was not included in his formalism, which may be important for the present spin-flip excitation processes, particularly for the (d,d') process. The extension of his expressions to the case including the spin-orbit distortion can readily be made by the use of standard DWBA formalism.[13] Therefore, here we give only a brief description of the generalization of the relevant theory to include (^{6}Li,^{6}Li′) scattering.

The DWBA amplitude of the reaction $A(a,b)B$ including the spin-orbit distortions is defined by

$$T_{fi}=\sum_{M_b' M_a'}\langle\chi^{(-)}_{M_b' M_b}(\vec{k}_f)\,|K_{M_B M_b', M_A M_a'}|\,\chi^{(+)}_{M_a' M_a}(\vec{k}_i)\rangle, \quad (1)$$

where $K_{M_B M_b', M_A M_a'}$, which is the same as K defined by Madsen,[1] is the nuclear transition matrix element

$$K_{M_B M_b, M_A M_a}(\vec{r}) = \langle\psi_{J_B M_B, T_B \tau_B}\psi_{J_b M_b, T_b \tau_b}\,|V|\,\psi_{J_a M_a, T_a \tau_a}\psi_{J_A M_A, T_A \tau_A}\rangle, \quad (2)$$

and V is the two-body nucleon-nucleon interaction potential,

$$V=\sum_{ij}\sum_{st} V_{st} f(r_{ij})(\vec{\sigma}_i\cdot\vec{\sigma}_j)^s(\vec{\tau}_i\cdot\vec{\tau}_j)^t, \quad (3a)$$

where s and t are the spin and isospin transfer, respectively. Corresponding to the Yukawa or Gaussian form of the radial shape of $f(r_{ij})$ the strength and the range parameter are defined by

$$V_{st}f(r_{ij})=\begin{cases} V^Y_{st}\exp(-\alpha r_{ij})/\alpha r_{ij}, \\ V^G_{st}\exp(-\beta r_{ij}^2). \end{cases} \quad (3b)$$

The distorted scattering waves are expressed by χ's in Eq. (1), and ψ's in Eq. (2) are the nuclear wave functions of target (A), projectile (a), residual nucleus (B) and ejectile (b), respectively. The total spin and its projection along the Z axis (isospin and its projection) are denoted by $JM(T\tau)$, respectively. The notations for the radial vector coordinates are shown in Fig. 1.

Equation (2) is expanded in terms of the transferred spin s, isospin t, and total spin j,

$$K_{M_B M_b, M_A M_a}(\vec{r}) = \sum_{jst} \sum_{j_1 j_2 \alpha_1 \alpha_2} S(jJ_AJ_B; j_1 j_2 \alpha_1 \alpha_2) S'(sJ_aJ_b; tT_aT_b)$$
$$\times \sum_{\mu\sigma\tau\beta_1\beta_2} (-)^{J_A - M_A}(J_A M_A J_B - M_B | j-\mu)(-)^{J_a - M_a}(J_a M_a J_b - M_b | s-\sigma)$$
$$\times (-)^{T} a^{-\tau} a(T_a \tau_a T_b - \tau_b | t-\tau)(-)^{(1/2)-\beta_1}(\tfrac{1}{2}\beta_1 \tfrac{1}{2} - \beta_2 | t-\tau) f_{js}(\vec{r}), \tag{4a}$$

where $f_{js}(\vec{r})$ is defined by

$$f_{js}(\vec{r}) = \sum_{\mu_1 \nu_1} (-)^{j_1 - \mu_1}(j_1 \mu_1 j_2 - \mu_2 | j-\mu)(-)^{(1/2)-\nu_1}(\tfrac{1}{2}\nu_1 \tfrac{1}{2} - \nu_2 | s-\sigma)$$
$$\times \langle \phi_{j_2 \mu_2} \phi_{\nu_2 \beta_2} | V_{an}^{st}(\vec{\sigma}_1 \cdot \vec{\sigma}_0)^s (\vec{\tau}_1 \cdot \vec{\tau}_0)^t | \phi_{j_1 \mu_1} \phi_{\nu_1 \beta_1} \rangle . \tag{4b}$$

The spectroscopic amplitudes S and S' in Eq. (4a) are the same as defined by Madsen.[1] The wave function $\phi_{j_1 \mu_1}(\phi_{j_2 \mu_2})$ in Eq. (4b) is that of the nucleon in target (residual) nucleus, respectively, and the $\phi_{\nu_1 \beta_1}(\phi_{\nu_2 \beta_2})$ is the product of spin and isospin part of the nucleon wave functions in projectile (ejectile) system, respectively. The suffixes ν and β denote the projections of its spin and isospin, respectively, and α in the S factor in Eq. (4a) corresponds to the projection of the isospin of the nucleon in the target system. In Eq. (4b), V_{an}^{st} is the projectile-(a)-nucleon-(n) interaction potential (same as $\bar{V}$ in Ref. 1) obtained by integrating over the projectile radial coordinate ξ,

$$V_{an}^{st}(r_{an}) = V_{st} \int d^3\xi g^2(\xi) f(r_{10}) , \tag{5}$$

where $g(\xi)$ is the radial part of the projectile wave function. If we assume a Gaussian wave function for $g(\xi)$, it is well known that the projectile-nucleon interaction potential takes a rather simple form; for the Gaussian interaction, the result is again Gaussian,[1] and for the Yukawa interaction, the result is approximately expressed by a Yukawa form outside the radius of the target nucleus,[14]

$$V_{an}^{st}(r_{an}) = \begin{cases} \bar{V}_{st}^{G} \exp(-\bar{\beta} r_{an}^2) , & \text{(6a)} \\ \bar{V}_{st}^{Y} \exp(-\bar{\alpha} r_{an})/\bar{\alpha} r_{an} , & \text{(6b)} \end{cases}$$

where

$$\bar{V}_{st}^{G} = V_{st}^{G}(1 + \beta\delta/\gamma^2)^{-3/2} ,$$
$$\bar{\beta} = \beta(1 + \beta\delta/\gamma^2)^{-1} \tag{7a}$$

and

$$\bar{V}_{st}^{Y} \simeq V_{st}^{Y} \exp(\alpha^2/18\gamma^2) , \quad \bar{\alpha} \simeq \alpha \text{ for } r_{an} > R_n . \tag{7b}$$

In Eq. (7), γ is the range parameter of wave function $g(\xi)$ and δ is the numerical factor depending on the projectile mass.[1] The approximate relations (7b) were found by numerical calculation[14] of Eq. (5). It is useful for the cases of strongly absorbed projectiles, like ^{6}Li, since the absorption eliminates the contribution from the inside region where the approximation becomes worse. In the present calculations, however, we use the relations (7b) for the (d, d') excitation also for the sake of simplicity.

The matrix element of the single-particle transition in Eq. (4b) is calculated by making the tensor expansion for the projectile-nucleon interaction V_{an}^{st},

$$V_{an}^{st}(r_{an}) = \bar{V}_{st} \sum_{lm} V_l(r, r_1) Y_{lm}^*(\hat{r}) Y_{lm}(\hat{r}_1) , \tag{8}$$

where $\bar{V}_{st}$ is $\bar{V}_{st}^{G}$ or $\bar{V}_{st}^{Y}$ defined by Eq. (6). Then the function $f_{js}(\vec{r})$ is expressed as follows:

$$f_{js}(\vec{r}) = 2 \sum_{lml_1 l_2} i^{l_1 - l_2} \bar{V}_{st} f_l(r) Y_{lm}^*(\hat{r}) \langle l_2 || Y_l || l_1 \rangle (-)^{j_1 - j_2 + j} \hat{j}_1 \hat{j}_2 \hat{s} (-)^{s-\sigma} (lms - \sigma | j\mu) \begin{pmatrix} l_1 & \frac{1}{2} & j_1 \\ l_2 & \frac{1}{2} & j_2 \\ l & s & j \end{pmatrix} D(\alpha\beta t) , \tag{9a}$$

where $D(\alpha\beta t)$ is defined as

$$D(\alpha\beta t) = (2\delta_{\alpha_1\beta_2}\delta_{\alpha_2\beta_1} - \delta_{\alpha_1\alpha_2}\delta_{\beta_1\beta_2})\delta_{t1} + \delta_{\alpha_1\alpha_2}\delta_{\beta_1\beta_2}\delta_{t0} , \tag{9b}$$

and the radial function $f_l(r)$ is defined as

$$f_l(r) = \int dr_1 r_1^2 \phi_{l_2}(r_1) V_l(r, r_1) \phi_{l_1}(r_1) . \tag{9c}$$

The expression for the differential cross section can be obtained from the standard DWBA formalism[13] and its explicit form is given in the Appendix.

The extension to the case of (^{6}Li, ^{6}Li′) excitation is straightforward if we assume a simple cluster model wave function for the ^{6}Li projectile. Here the ^{6}Li ground state is assumed to have the $\alpha + d$ cluster structure. The ^{6}Li nucleus has also a

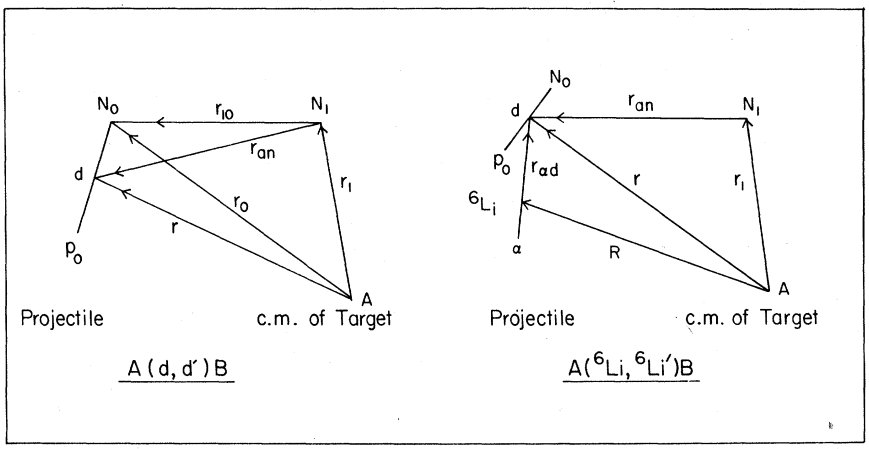

FIG. 1. Notations for the space coordinate vectors. The figure on the left-hand side is for the $d+A$ scattering system. The relative coordinate between d and A is denoted by $\vec{r}$. The figure on the right-hand side is for the ^{6}Li$+A$ scattering system where the $d+A$ subsystem is contained, since the ^{6}Li$=d+\alpha$ cluster description was assumed here for the projectile. The relative coordinate between ^{6}Li and A is denoted by $\vec{R}$.

fraction of ^{3}He$+t$, but one takes the risk of double counting if one sums the reaction amplitude arising from this fraction to that of the $\alpha+d$ fraction, since both fractions are not completely orthogonal. If the simple LS-shell model is used for describing the ^{6}Li ground state, it can be proved that the ^{3}He $+t$ fraction has a complete overlap with the $\alpha+d$ fraction.[15]

The spin-flip $s=1$ transition is thus induced by the d cluster, whereas the α cluster is assumed to be a spectator. The nucleon transition matrix element in Eq. (2) is now replaced by the following expression:

$$F(\vec{R})=\int d\vec{r}_{\alpha d}\phi_0^*(\vec{r}_{\alpha d})K_{M_BM_b,M_AM_a}(\vec{r})\phi_0(\vec{r}_{\alpha d})\ , \quad (10)$$

where $K(\vec{r})$ is the nuclear matrix element defined by Eq. (2) and $\phi_0(\vec{r}_{\alpha d})$ is the s-state wave function for the relative motion between α and d clusters in ^{6}Li. The integral of Eq. (10) can be performed by introducing the tensor expansion method[16] as in Eq. (8) for the function $f_l(r)Y_{lm}^*(\hat{r})$ which appears in Eq. (9a). We define the function

$$I_{lm}(\vec{R})=\int d\vec{r}_{\alpha d}\,|\phi_0(\vec{r}_{\alpha d})|^2 f_l(r)Y_{lm}^*(\hat{r})$$
$$=\frac{1}{2}\sum_\lambda\begin{pmatrix}2l+1\\2\lambda\end{pmatrix}^{1/2}(l\,\hat{-}\,\lambda)/\hat{l}\,(l0l-\lambda0\,|\,l0)Y_{lm}^*(\hat{R})R^{l-\lambda}\int dr_{\alpha d}\,r_{\alpha d}{}^2(\tfrac{4}{6}r_{\alpha d})^\lambda g_\lambda(R,r_{\alpha d})\phi_0{}^2(r_{\alpha d}), \quad (11a)$$

where we used the relation $\vec{r}=\vec{R}+\frac{4}{6}\vec{r}_{\alpha d}$ (see Fig. 1), and the g_λ is defined as the expansion coefficient of the radial function $f_l(r)r^{-l}$,

$$f_l(r)r^{-l}=\sum_\lambda\frac{2\lambda+1}{2}g_\lambda(R,r_{\alpha d})P_\lambda(\cos\theta), \quad (11b)$$

and θ is the angle between the two vectors $\vec{R}$ and $\vec{r}_{\alpha d}$. The radial part of the cluster wave function is denoted by $\phi_0(r_{\alpha d})$. Inserting the explicit form of the Clebsch-Gordan coefficient[17] in Eq. (11a),

$$I_{lm}(\vec{R})=\frac{1}{2}\sum_{\lambda=0}^{l}R^{l-\lambda}\int dr_{\alpha d}\,r_{\alpha d}{}^2(\tfrac{4}{6}r_{\alpha d})^\lambda g_\lambda(R,r_{\alpha d})$$
$$\times\phi_0{}^2(r_{\alpha d})Y_{lm}^*(\hat{R}). \quad (12a)$$

Therefore, the nuclear transition matrix element $F(\vec{r})$ for the (^{6}Li,^{6}Li′) spin-flip transition has the same expression as the $K_{M_BM_b,M_AM_a}(\vec{r})$ given by Eq. (4) after replacing the quantity $f_l(r)Y_{lm}^*(\hat{r})$ by the new function $I_{lm}(\vec{R})$ obtained above. That is, the radial factor $f_l(r)$ is now replaced by

$$f_l(R)=\tfrac{1}{2}\sum_{\lambda=0}^{l}R^{l-\lambda}\int dr_{\alpha d}\,r_{\alpha d}{}^2(\tfrac{4}{6}r_{\alpha d})^\lambda g_\lambda(R,r_{\alpha d})\phi_0{}^2(r_{\alpha d}). \quad (12b)$$

From the expressions, it is easy to see that the angular momentum selection rule for the (^{6}Li,^{6}Li′) spin-flip transition is exactly the same as that of the (d,d') transition. This result arises from the present S-state assumption for the relative motion between the α and d cluster in ^{6}Li.

III. PHYSICAL PARAMETERS USED IN THE CALCULATIONS

Microscopic studies of the ^{12}C$(d,d')^{12}$C scattering leading to the 4.43-MeV (2^+), 7.66-MeV (0^+), and 9.64-MeV (3^-) states have been reported

TABLE I. Range parameters of interaction potentials used for present calculations. The range parameters are defined by Eq. (3) for the nucleon-nucleon interaction and by Eq. (6) for the projectile-nucleon interaction.

Nucleon-nucleon interaction			Projectile-nucleon interaction (d,d')		$(^3\mathrm{He},^3\mathrm{He}')$	
Gaussian	β (fm^{-2})	Range (fm)	$\bar{\beta}$ (fm^{-2})	Range (fm)	$\bar{\beta}$ (fm^{-2})	Range (fm)
	0.745	1.16	0.35	1.7 (G-1.7)	0.25	2.0 (G-2.0)
	0.408	1.57	0.25	2.0 (G-2.0)	0.20	2.25 (G-2.25)
Yukawa	α (fm^{-1})	Range (fm)	$\bar{\alpha}$ (fm^{-1})	Range (fm)	$\bar{\alpha}$ (fm^{-1})	Range (fm)
	1.0	1.0	1.0	1.0 (Y-1.0)	1.0	1.0 (Y-1.0)
	0.83	1.2	0.83	1.2 (Y-1.2)	0.83	1.2 (Y-1.2)

by Hinterberger *et al.*[12] at $E_d = 52$ MeV. The interaction potential used was Gaussian and its range parameter was $\bar{\beta} = 0.27$ fm^{-2} (1.9-fm range) for the projectile-nucleon interaction [see Eq. (6a)], which corresponds to the range parameter $\beta = 0.35$ fm^{-2} (1.7-fm range) of the nucleon-nucleon interaction using $\gamma = 0.566$ fm^{-1} and $\delta = 0.25$ for the deuteron wave function. We used a smaller range parameter $\gamma = 0.402$ fm^{-1} taken from Madsen[1] and used $\beta = 0.408$ fm^{-2} (1.57-fm range), so that the effective deuteron-nucleon interaction range becomes $\bar{\beta} = 0.25$ fm^{-2} (2.0-fm range). The range parameter dependence of the differential cross section was studied in the present analysis and it was found that a larger range parameter $\beta = 0.745$ fm^{-2} (1.2-fm range) provides a better fit to the data for the 12.71-MeV (1^+) state excitation. Therefore we will discuss the results obtained using these two different range parameters, $\beta = 0.408$ and 0.745 fm^{-2}, for the Gaussian nucleon-nucleon interaction.

Ball and Cerny[7] studied the ^{12}C(^{3}He,^{3}He′)^{12}C scattering leading to the 12.71-MeV (1^+) state as well as other particle-hole states in $1p$-shell nuclei at $E_{^3\mathrm{He}} = 49.8$ MeV. They used approximate relations (6b) and (7b) for the Yukawa interaction potential and found the range parameter $\bar{\alpha} \simeq \alpha = 0.83$ fm^{-1} (1.2-fm range) to provide good fits to the experimental angular distribution. This interaction potential was adopted here and the interaction strength V_{st}^{Y} obtained from the present analysis of the ^{12}C$(d,d')^{12}$C 12.71-MeV (1^+) state excitation is compared with that determined in Ref. 7. We also carried out calculations with $\alpha = 1.0$ fm^{-1}, since it is a typical range of the Yukawa form used for usual microscopic analyses of the (p,p') inelastic scattering. The range parameter γ of the ^{3}He wave function is chosen to be 0.29 fm^{-1} as in Ref. 7.

Thus in the present calculations, four different types of interaction potentials were used for the analyses of (d,d') and (^{6}Li,^{6}Li′) data as well as for the reanalyses of (^{3}He,^{3}He′) data. In Table I, all range parameters used in this work are summarized. The Gaussian interaction with range 1.7 fm and the Yukawa interaction with range 1.0 fm are hereafter referred to as G-1.7 and Y-1.0, respectively.

The distorting potential for the (d,d') calculations at the incident energy of 28 MeV was taken from Perrin *et al.*[18] which was found to fit the ^{12}C$+d$ elastic scattering angular distribution as well as polarization data for the incident energies of 20.5, 25.2, and 29.5 MeV. We used the set designated in Ref. 18 as GM2 (see the caption to Fig. 2). The corresponding elastic scat-

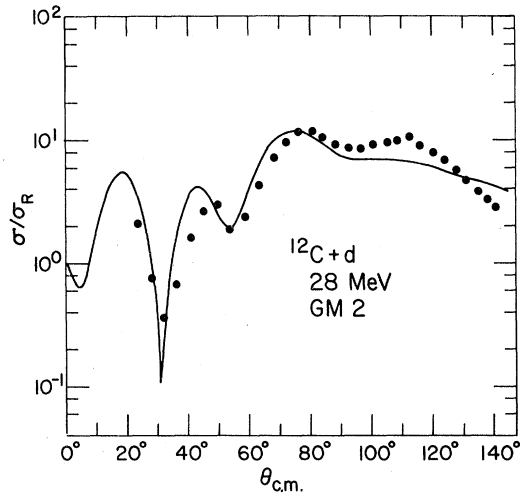

FIG. 2. Rutherford ratio of the elastic angular distribution of the ^{12}C$+d$ scattering at 28 MeV. The experimental data, shown by the solid circles, are provided from Refs. 5 and 6. The optical model calculation, shown by the solid line, was done using the parameter set GM2 from Ref. 18. The parameters are $V = 109$ MeV, $r_0 = 0.9$ fm, and $a = 0.82$ fm for the real potential; $V_{LS} = 8.5$ MeV, $r_{LS} = 0.9$ fm, and $a_{LS} = 0.55$ fm for the spin-orbit potential, $W_D = 3.125 + 0.209E$(=8.98) MeV, $r_D = 2.1 - 0.022E$(=1.48) fm, and $a_D = 0.745$ fm for the Woods-Saxon derivative type imaginary potential, where W_D and r_D are dependent on incident energy E and the values inside the parentheses are for $E = 28$ MeV.

tering differential cross section calculated for $E_d = 28$ MeV is shown in Fig. 2 and compared with the data. For the (^{6}Li, ^{6}Li′) calculation, the distorting potential employed by Bindal *et al.*[19] was used for the ^{12}C + ^{6}Li elastic scattering (see the caption to Fig. 4). The radial wave function $\phi_0(r_{\alpha d})$ [see Eq. (11a)] was obtained using the usual separation energy method. The corresponding Woods-Saxon bound-state parameters were $R_0 = 1.9$ fm, $a = 0.65$ fm, and $V_0 = 77.2$ MeV. This potential gives almost the same radial shape as that predicted by the resonating group method for the ^{6}Li ground state.[20] The wave function of the 12.71-MeV ($1^+, T = 0$) state of ^{12}C was taken to be $(1p_{3/2}^{-1}1p_{1/2})$ configuration[21] where other small components and possible admixtures of isospin[22-24] were ignored. The wave functions of $1p_{3/2}$ and $1p_{1/2}$ single-particle states in ^{12}C were calculated using the Woods-Saxon potential with the separation energy method, assuming $r_0 = 1.25$ fm and $a = 0.65$ fm. The separation energies used were determined from the corresponding reaction Q value assuming neutron excitation. The separation energies of neutron and proton in the ^{12}C ground state are 18.7 and 16.0 MeV, respectively. Therefore the cross sections calculated here may be lower estimates.

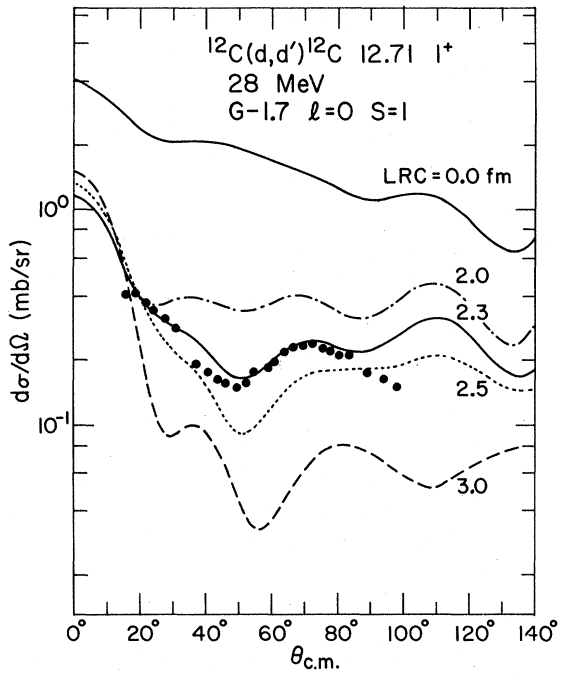

FIG. 3. The lower radial cutoff (LRC) parameter dependence of the calculated angular distribution of (d, d') at 28 MeV leading ^{12}C to the 12.71-MeV ($1^+, T = 0$) state. The experimental data, shown by the solid circles, are taken from Refs. 5 and 6. Theoretical $l = 0$ angular distributions were calculated using the Gaussian type 1.7-fm range projectile-nucleon interaction potential and the results are shown for the five different cutoff cases. They are normalized by use of $\overline{V}_{10} = 12.1$ MeV (see also Table II).

IV. RESULTS OF CALCULATIONS AND SPECIFIC DISCUSSIONS

A. ^{12}C(d,d')^{12}C 12.71 MeV (1^+) at 28 MeV

Calculated (d, d') angular distributions and experimental data[5,6] leading to the ^{12}C 12.71-MeV ($1^+, T = 0$) state are shown in Fig. 3, where the Gaussian interaction with 1.7-fm range (G-1.7) was used. Since the present incident energy is rather low, there exists a mismatch problem[25] between the momenta of the initial and final scattering states, and consequently a lower radial cutoff (LRC) was found to be necessary in the DWBA calculation to reproduce the structure of the angular distribution observed.

For such mismatch cases, it is well know that the effects arising from nonlocalities[26] (NL) of the optical potential and the bound state potential are quite considerable, particularly in the light-ion reactions, since contributions from the nuclear interior to the DWBA amplitude is appreciably enhanced if such NL effects are ignored. The calculated angular distribution with LRC therefore effectively simulates the NL corrections. This was checked using NL parameters $\beta = 0.54$ for the distorting potential of the $d + ^{12}$C systems and $\beta = 0.85$ for the bound-state potential of p-shell nucleons. The obtained angular distribution was quite similar to that obtained by using LRC = 2.0 fm without such corrections, but the change in magnitude of the cross section was different, i.e., the reduction due to the NL corrections is by a factor of 1.6, whereas that due to LRC is by a factor of 4.6. The NL correction is, however, not enough to reproduce the observed shape of the angular distribution (see the case of LRC = 2.0 in Fig. 3). One of the reasons arises from a predominant $l = 0$ transfer for such an 1^+ state excitation (see Sec. IV B), where contributions from nuclear interior are quite enhanced owing to the finite nature of the $l = 0$ form factor at the origin.

Therefore, we here simply use only LRC instead of NL corrections when we consider the fits of calculated angular distributions to the data. The cutoff radius was changed in the calculation up to 3 fm and a reasonable fit was obtained for LRC = 2.3 fm. The cross section was reduced by about a factor of 5 with this cutoff. All calculated cross sections shown in Fig. 3 are normalized using the same constant factor found for the normalization of the case of LRC = 2.3 fm. The angular distributions calculated using three other different interaction potentials (see Table I) are shown at the upper portion

of Fig. 4 together with the case of the G-1.7. For all calculations, a radial cutoff 2.3 fm was used. The case of G-1.7 gives the best fit to the observed data and it was found so from other choices of LRC parameters.

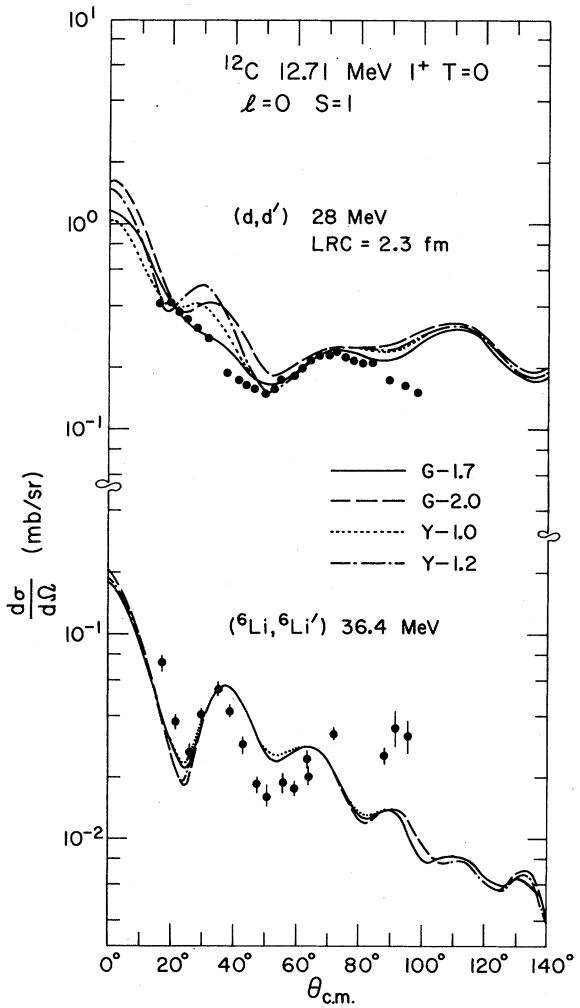

FIG. 4. Angular distributions of the (d,d') process at 28 MeV (shown at the upper part) and the (^{6}Li, ^{6}Li′) process at 36.4 MeV (shown at the lower part) leading to the ^{12}C 12.71-MeV ($1^+, T=0$) state. The experimental data for (^{6}Li, ^{6}Li′) were taken from Ref. 19. The four different curves show the $l=0$ partial angular distributions calculated using four different interaction potentials, which are annotated in the figure as G-1.7 for the Gaussian type 1.7-fm range potential, etc. (see also Table I). The calculated cross sections are normalized by using the strength $\overline{V}_{10}$ given in Table II. The distorting potentials used for the (^{6}Li, ^{6}Li′) process were the same as those from Ref. 19. The parameters are $V=85.2-0.64E_{c.m.}$ MeV, $r_0=0.97$ fm, and $a=0.735$ fm for the real potential, $W=-6.4+0.96E_{c.m.}$ MeV, $r_0'=1.25$ fm, and $a'=0.386$ fm for the volume type imaginary potential, and $r_c=1.35$ fm, where all radius parameters are defined such as multiplication by $(A_1^{1/3}+A_2^{1/3})$ gives the potential radius, with the exception of the case of the (d,d') in the caption to Fig. 1.

The interaction strengths extracted from the normalization of calculated cross sections to experimental data at the $\theta_{c.m.}=20°$ are summarized in Table II. The normalizations provide the projectile-nucleon interaction strengths $\overline{V}_{10}^{G}$ or $\overline{V}_{10}^{Y}$ defined by Eqs. (6) and (7). For the (^{6}Li, ^{6}Li′) reaction, these are the strengths of the interaction between the d cluster in ^{6}Li and the nucleon in ^{12}C. The obtained strengths were reduced to the nucleon-nucleon interaction strength V_{10}^{G} or V_{10}^{Y} using Eq. (7). Assuming the equivalence of the volume integral of the interaction potential, the equivalent strength V_{10}(Y-1.0) to the strength of the Yukawa form with 1.0-fm range can be obtained by using the following relations:

$$V_{st}(\text{Y-1.0}) = \begin{cases} C(\alpha{:}1.0)\,\dfrac{v(\alpha{:}1.0)}{v(\alpha{:}1.2)}\,\overline{V}_{st}^{Y}(\overline{\alpha}), & \text{(13a)} \\ C(\alpha{:}1.0)\,\dfrac{v(\alpha{:}1.0)}{v(\overline{\beta})}\,\overline{V}_{st}^{G}(\overline{\beta}), & \text{(13b)} \end{cases}$$

where the v's are the volume integrals of Yukawa or Gaussian interaction form,

$$\int d\vec{r}_{ij} f(r_{ij}) = \begin{cases} 4\pi/\alpha^3 = v(\alpha), \\ (\pi/\beta)^{3/2} = v(\beta), \end{cases}$$

and $C(\alpha{:}1.0)$ is $\exp(-1/18\gamma^2)$, the conversion factor of the projectile-nucleon interaction to the nucleon-nucleon interaction with range parameter $\alpha=1.0$ fm^{-1} for Yukawa potential [see Eq. (7b)]. Equations (13) correspond to one way of conversion; that is, first the strength of projectile-nucleon interaction is converted to that of an equivalent projectile-nucleon Yukawa interaction with 1.0-fm range, and then to that of the nucleon-nucleon Yukawa interaction. There is another way of conversion; first to convert to the nucleon-nucleon interaction and then reduce it to the equivalent Yukawa 1.0-fm interaction. These two different ways give different results, and for the (d,d') case, the latter gives about 10 or 40% larger strength corresponding to Yukawa or Gaussian types of interaction, respectively. Equations (13) were used for all reactions and excitations discussed in this paper to derive an equivalent strength V_{st}(Y-1.0).

From Table II, it can be seen that the spin-spin interaction strengths V_{10}(Y-1.0) thus obtained from the (d,d') process at 28 MeV are almost constant at 8.28 MeV on the average without cutoff (LRC = 0.0 fm) and 20.2 MeV with LRC = 2.3 fm.

B. ^{12}C(^{6}Li,^{6}Li′)^{12}C, 12.71 MeV (1^+) at 36.4 MeV

Since the incident energy of 36.4 MeV is not so high in comparison with the Q value of 12.71 MeV,

TABLE II. Interaction strengths obtained from the ^{12}C 12.71 MeV ($1^+, T=0$) state excitation calculation using four different interaction potentials with $1p_{3/2} \rightarrow 1p_{1/2}$ transition picture.

^{12}C 12.71 MeV (1^+)			$\bar{V}_{10}$[a] (MeV)	V_{10}[b] (MeV)	V_{10}(Y-1.0)[c] (MeV)
(d, d') 28 MeV	LRC = 0.0	Y-1.0	11.4	8.09	8.09
		Y-1.2	7.31	5.76	8.97
		G-1.7	4.90	15.5	7.56
		G-2.0	3.39	7.06	8.53 (8.28)[d]
	LRC = 2.3	Y-1.0	28.3	20.1	20.1
		Y-1.2	17.7	14.0	21.7
		G-1.7	12.1	38.2	18.7
		G-2.0	8.14	17.0	20.5 (20.2)[d]
(^{6}Li, ^{6}Li′) 36.4 MeV		Y-1.0	12.2	8.67	8.67
		Y-1.2	7.60	5.99	9.32
		G-1.7	5.35	16.9	8.26
		G-2.0	3.44	7.17	8.65 (8.73)[d]
(^{3}He, ^{3}He′) 49.8 MeV		Y-1.0	20.6	10.7	10.7
		Y-1.2	11.9	7.51	10.6
		G-2.0	5.54	27.5	10.1
		G-2.25	3.76	11.2	9.89 (10.3)[d]

[a]Strength $\bar{V}^G_{st}$ or $\bar{V}^Y_{st}$ of projectile-nucleon interaction [see Eqs. (6) and (7)] for $s=1$ and $t=0$. For (^{6}Li, ^{6}Li′), strength of d cluster and nucleon interaction.

[b]Strength V^G_{st} or V^Y_{st} of original nucleon-nucleon interaction [see Eq. (3)] for $s=1$ and $t=0$.

[c]Strength converted to the Yukawa 1.0-fm range interaction using volume integral discussed in the text.

[d]Average strength.

there might be a momentum mismatch problem here also which was very serious in the case of (d, d') at 28 MeV. The nuclear interior contribution was examined by changing the LRC parameter up to 5 fm for every 0.5-fm step. It was found that the shape of the angular distribution was quite stable and that the cross section decreased by only a factor of 3 with LRC = 3.0 fm, which is rather small in comparison with those found in the analysis of (d, d') at 28 MeV. Such suppressed contribution from the nuclear interior in the case of (^{6}Li, ^{6}Li′) scattering may be caused by the smaller amplitude and large cancellation due to the more frequent oscillations of the distorted waves compared with the corresponding situation for (d, d') scattering.

The results of the calculations are shown in the bottom portion of Fig. 4 after normalizing them to the data observed at $\theta_{\text{c.m.}} = 35°$. The radial cutoff was not used. Differences in the shapes of angular distributions arising from the use of different interaction potentials are less than those appearing in the (d, d') excitation. This reduced sensitivity in the (^{6}Li, ^{6}Li′) excitation to the shape of the interaction potential obviously comes from the fact that the form factor is more smeared out owing to the additional integration over the ^{6}Li cluster model wave function $\phi_0(r_{\alpha d})$ [see Eq. (11a) and Fig. 1].

The interaction strengths derived are given in Table II and the equivalent strength V_{10}(Y-1.0) was found to be 8.73 MeV on the average, which is quite consistent with that determined in the (d, d') analysis without cutoff.

For the present unnatural parity 1^+ state excitation, there exists two possible transferred angular momenta, $l=0$ and 2 [see Eq. (9a)], and only the $l=0$ part of the cross sections was discussed above. The $l=2$ cross sections are shown in Fig. 5 and they are compared with those of the $l=0$ transfer for the (d, d') and (^{6}Li, ^{6}Li′) excitation. The same interaction strength was used for normalizing the $l=2$ cross section as was used for normalizing each $l=0$ cross section to the experimental data. The $l=2$ cross section is about one order of magnitude smaller in the (d, d') and about 50 times smaller in the (^{6}Li, ^{6}Li′) excitation. Since the spin-orbit distortion was used in the present (d, d') calculation, these two transition amplitudes should be summed coherently. However, since the $l=2$ component is relatively small, it was neglected.

It may be argued that such a small contribution of the $l=2$ transfer is physically reasonable. In a classical picture, the $l=2$ transfer corresponds to a process of double flips, the flip of the orbital rotation of the valence nucleon as well as the flip of the intrinsic spin, whereas the $l=0$ transfer is

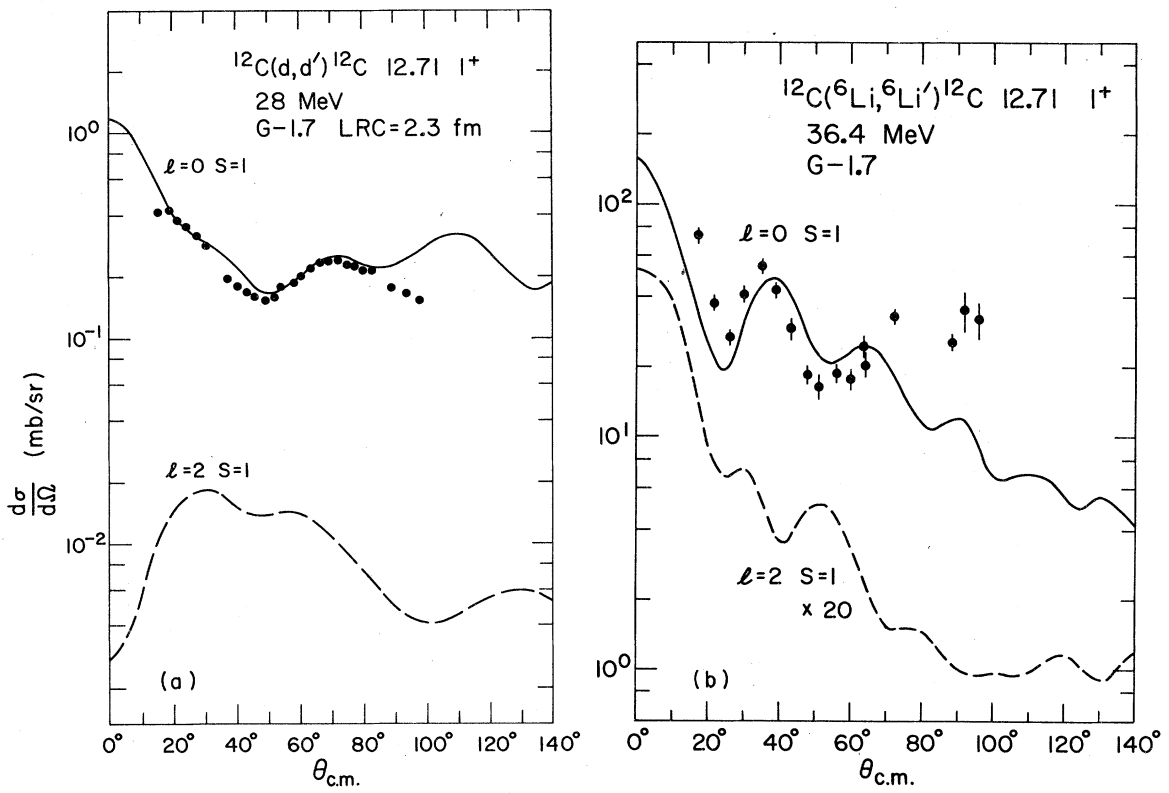

FIG. 5. (a) Comparison of the calculated $l=2$ partial cross section with that of the $l=0$ for (d,d') at 28 MeV leading to the ^{12}C 12.71-MeV ($1^+, T=0$) state. The calculations were performed using the Gaussian type 1.7-fm range projectile-nucleon interaction potential and the lower radial cutoff 2.3 fm was used for both $l=0$ and $l=2$ cases. The $l=2$ cross section is normalized using the same strength $\overline{V}_{10}=12.1$ MeV used for the $l=0$ cross section. (b) Comparison of the calculated $l=2$ partial cross section with that of the $l=0$ for the (^{6}Li, ^{6}Li') process at 36.4 MeV leading to the ^{12}C 12.71-MeV ($1^+, T=0$) state. In the figure, the $l=2$ cross section is normalized using the same $\overline{V}_{10}$ used for the $l=0$ cross section and then multiplied by an arbitrary factor of 20. See also the caption to Fig. 5(a).

a nonflip process for the orbital rotation. The other evidence for suppression of the $l=2$ transfer is a concentrated $M1$ γ decay [with a branching ratio of 83.3% (Ref. 22)] from this state to the ground state.

C. ^{12}C(^{3}He,^{3}He')^{12}C 12.71 MeV (1^+) at 49.8 MeV

In the calculations, the distorting potential parameter set F given by Ball and Cerny[7] was used. The results are shown in Fig. 6. The case of the Y-1.2 potential without LRC (LRC=0.0 shown by dot-dashed line at the upper part) corresponds to that of Ball and Cerny.[7] All calculated cross sections were normalized to the data at the angle $\theta_{c.m.}=20°$ and the extracted interaction strengths are summarized in the last four rows of Table II. The equivalent nucleon-nucleon interaction strength V_{10}(Y-1.0) obtained from the use of Y-1.2 potential is 10.6 MeV and this value is the same as that obtained in Ref. 7 (see comments on Ref. 7).

From Table II, one can conclude that the present four different interaction potentials used in the (^{3}He,^{3}He') analysis give an almost constant strength, about 10 MeV, for the equivalent nucleon-nucleon potential V_{10}(Y-1.0). However, there exist problems as seen in Fig. 6, particularly at forward angles. It was found that the introduction of LRC does not improve the quality as is evident from the lower portion of Fig. 6 where LRC=2.0 fm was used. The calculated cross section is reduced by a factor of 2 with this cutoff. The contribution from the $l=2$ transfer was estimated and the result is shown in Fig. 7. The $l=2$ cross section is about two orders of magnitude smaller around the angle $\theta_{c.m.}=20°$ than that of the $l=0$ transfer, consistent with those found in the (d,d') and (^{6}Li,^{6}Li') scatterings discussed in Sec. IV B. Therefore this $l=2$ component arising from the central $(\vec{\sigma}\cdot\vec{\sigma})$ type interaction does not appear to be the source of the present discrepancy at forward angles.

D. ^{12}C 4.43-MeV (2^+) state excitations

Microscopic studies of this state have been reported by Hinterberger *et al.*[12] from (d,d') scattering at $E_d = 52$ MeV and by Ball and Cerny[7] from (^{3}He,^{3}He′) scattering at $E_{^3\mathrm{He}} = 49.8$ MeV. Angular distributions calculated considering only the $1p_{3/2} \rightarrow 1p_{1/2}$ single-particle transition are shown in Fig. 8 and they are compared with the observed data. For the 28-MeV excitation, the interaction potential G-1.7 gives an overall good fit to the shape of the observed data. This result is consistent with that found in the 12.71-MeV (1^+) excitation. While for the 52-MeV case the potential G-2.0, which is very close to the G-1.92 (1.7-fm range of nucleon-nucleon Gaussian type interaction) used in the analysis of Hinterberger *et al.*,[12] gives the best fit. The reason for this energy dependence of the interaction potential is not well understood.

For the (^{3}He,^{3}He′) process, the Gaussian type interaction potential gives a sharp oscillatory angular distribution thereby reproducing the deep valley around the angle $\theta_{\mathrm{c.m.}} = 25°$, while the Yukawa potential gives a rather structureless angular distribution. The calculated angular distributions do not show satisfactory fits, which was also the case for the 12.71-MeV (1^+) state excitation by (^{3}He,^{3}He′) discussed in Sec. IV C.

The interaction strengths were obtained by normalizing the calculated results to the data as shown in Fig. 8, and are summarized in Table III. The equivalent Wigner part of the interaction

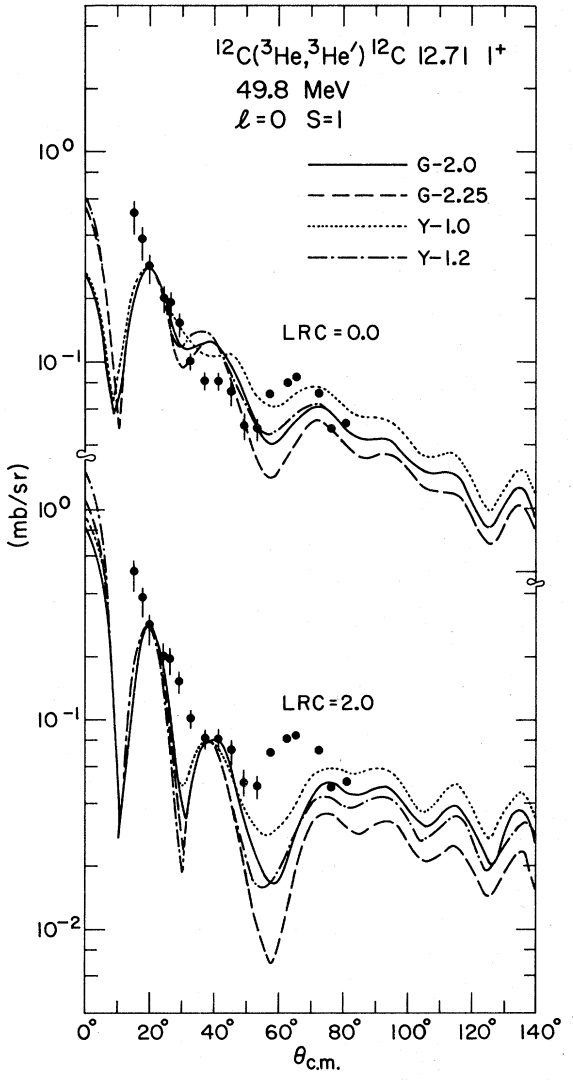

FIG. 6. Angular distribution of the (^{3}He,^{3}He′) process leading to the ^{12}C 12.71-MeV ($1^+, T = 0$) state at 49.8 MeV. Four different curves show the calculated $l = 0$ partial angular distributions corresponding to the four different projectile-nucleon interaction potentials used in the calculation, e.g., G-2.0 indicates the use of Gaussian type 2.0-fm range potential, etc. (see also Table I). The cases without lower radial cutoff and with a cutoff at 2.0 fm are shown. The experimental data are taken from Ref. 7.

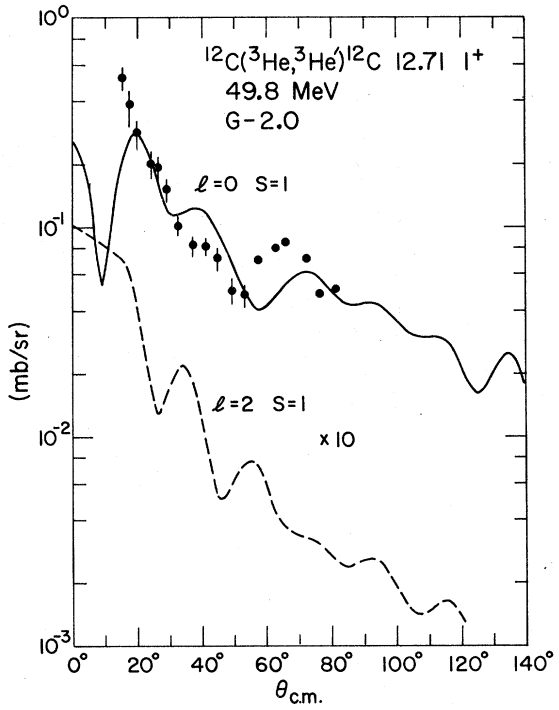

FIG. 7. The $l = 2$ partial angular distribution is compared with that of the $l = 0$ for the (^{3}He,^{3}He′) process at 49.8 MeV leading to the ^{12}C 12.71-MeV ($1^+, T = 0$) state. The Gaussian type 2.0-fm range potential was used for the projectile-nucleon interaction. The calculated cross sections are normalized using the same strength $\overline{V}_{10}$ given in Table II. For the $l = 2$ partial angular distribution, an additional renormalization was done by multiplying by a factor of 10.

strength V_{00}(Y-1.0) was obtained by using Eqs. (13). The strength of 85.9 MeV for the G-2.0 potential from the (d,d') analysis at 52 MeV is a little different from the result of 66 MeV obtained by Hinterberger *et al.*[12] using the G-1.92 potential, mainly owing to the different range parameter γ of the deuteron wave function (here we used $\gamma = 0.402$ fm^{-1} and they used 0.566 fm^{-1}, see also Sec. III). The equivalent strength of V_{00}(Y-1.0) = 92.4 MeV obtained from the (^{3}He,^{3}He′) analysis using the Y-1.2 potential is very close to the value of 92.7 MeV obtained by Ball and Cerny[7] even using the different distorting potential parameter set (see also Sec. IV C). The present analyses of three different reactions provide a quite consistent strength V_{00}(Y-1.0) of the equivalent interaction from four different interaction potentials: on the average 93.4 MeV for the (d,d') process at 28 MeV, 106 MeV from the (d,d') process at 52 MeV and 82.6 MeV from the (^{3}He,^{3}He′) process (see the last column in Table III).

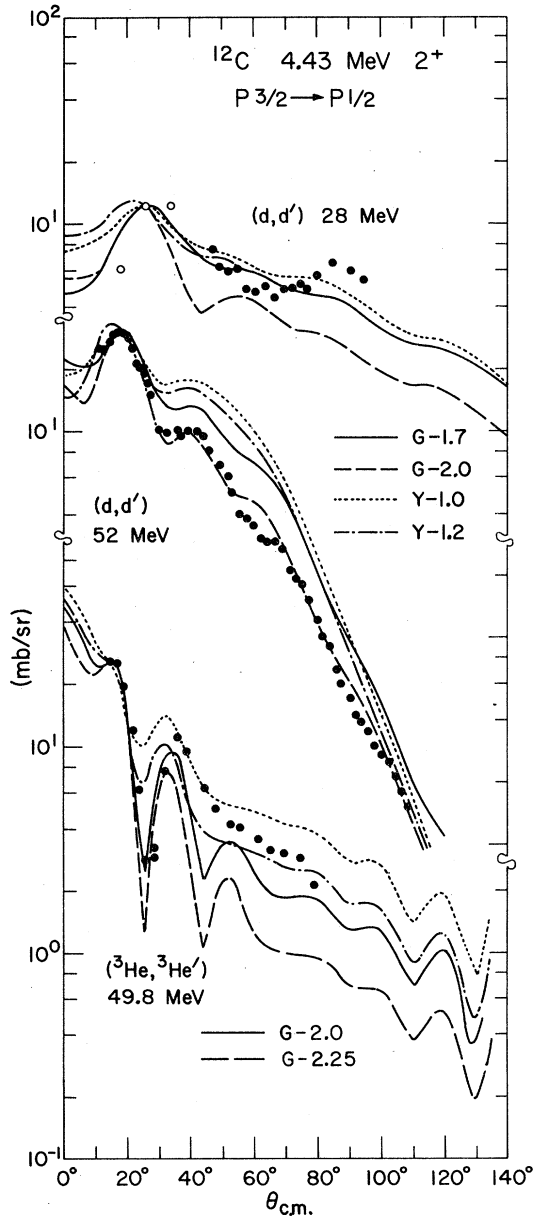

FIG. 8. Angular distributions of three different processes to excite the ^{12}C 4.43-MeV (2$^+$) state: (d,d') at 28 MeV, (d,d') at 52 MeV, and (^{3}He,^{3}He′) at 49.8 MeV. The experimental data are taken from Ref. 6 for the first three points shown by the open circles and from Ref. 5 for other solid circles in (d,d') at 28 MeV, from Ref. 12 for (d,d') at 52 MeV and from Ref. 7 for (^{3}He,^{3}He′). Four different curves show the results of calculations using the four different interaction potentials (see Table I). The single-particle $1p_{3/2} \rightarrow 1p_{1/2}$ transition process was assumed. The calculated cross sections are normalized using the strength $\bar{V}_{00}$ given in Table III.

V. DISCUSSION

The equivalent $(\vec{\sigma}\cdot\vec{\sigma})$ type interaction strength V_{10}(Y-1.0) was consistently obtained in the present analysis of the ^{12}C 12.71-MeV (1$^+$) state excitation by various processes, i.e., 8.28 MeV from the (d,d'), 8.73 MeV from (^{6}Li,^{6}Li′), and 10.3 MeV from (^{3}He,^{3}He′), on the average (see Table II). Owing to a momentum mismatch problem in the (d,d') at 28 MeV, LRC was necessary to reproduce the shape of the angular distribution observed. The interaction strength was increased to 20.2 MeV for the (d,d') process when the cutoff at 2.3 fm was used to fit the shape. Therefore (d,d') data at higher incident energies are quite desirable to check whether the strength of about 10 MeV will result again without the ambiguity of radial cutoff, since the momentum mismatch problem is expected to be less severe there.

In the present microscopic analyses, we employed only the $(\vec{\sigma}\cdot\vec{\sigma})$ type central potential, but we did not consider contributions from tensor forces or exchange processes. Such interactions of increasing complexity may not be so important[27-29] at least for analyses of the (p,p') excitation at high incident energies (100–200 MeV). However, the (p,p') experimental data at around 50 MeV leading to the ^{12}C 12.71-MeV (1$^+$, $T=0$) state and the 15.11-MeV (1$^+$, $T=1$) state show rather anomalous shapes in their angular distributions.[8,9] A broad peak at forward angles like an $l=2$ transition was seen, which is contrary to the prediction of the predominant $l=0$ transition if we use the $(\vec{\sigma}\cdot\vec{\sigma})$ central interaction. In addition to this, the angular distribution of the $T=0$ state transition showed a backward rise beyond $\theta_{c.m.}=100°$ in contrast to a sharp falloff in the $T=1$ state transition.

Love and Parish[11] investigated the effects of the

TABLE III. Interaction strengths required to produce the observed cross section exciting the ^{12}C 4.43-MeV (2^+) state using $1p_{3/2} \rightarrow 1p_{1/2}$ single-particle excitation.

^{12}C 4.43 MeV (2^+)		$\bar{V}_{00}$ [a] (MeV)	V_{00} [b] (MeV)	V_{00}(Y-1.0) [c] (MeV)
(d,d') 28 MeV	Y-1.0	119	84.4	84.4
	Y-1.2	80.1	63.0	98.1
	G-1.7	60.3	191	93.2
	G-2.0	38.9	81.0	97.7 (93.4) [d]
(d,d') 52 MeV	Y-1.0	146	104	104
	Y-1.2	94.2	74.2	116
	G-1.7	66.2	209	102
	G-2.0	41.2	85.9	104 (106) [d]
(^{3}He,^{3}He') 49.8 MeV	Y-1.0	177	91.8	91.8
	Y-1.2	103	65.1	92.4
	G-2.0	43.3	215	79.7
	G-2.25	25.4	75.5	66.7 (82.6) [d]

[a] Strength $\bar{V}_{st}^G$ or $\bar{V}_{st}^Y$ of projectile-nucleon interaction [see Eqs. (6) and (7)] for $s=1$ and $t=0$. For (^{6}Li,^{6}Li'), strength of d cluster and nucleon interaction.

[b] Strength V_{st}^G or V_{st}^Y of original nucleon-nucleon interaction [see Eq. (3)] for $s=1$ and $t=0$.

[c] Strength converted to the Yukawa 1.0-fm range interaction using volume integral discussed in the text.

[d] Average strength.

tensor force for the 15.11-MeV ($1^+, T=1$) state excitation, and they found that the enhanced $l=2$ transfer component arising from the tensor force is capable of reproducing such a broad peak at the forward angles. Mori[10] investigated the exchange (knockon) process for excitation of the 12.71-MeV ($1^+, T=0$) state, and he pointed out an important contribution of the unnatural parity $l=1$ transfer component, resulting in a broad peak at forward angles by the sum of the $l=1$ and the ordinary $l=0$ transfer components. The increasing trend at the backward angles is still an open question. The exchange process was also investigated by Love and Satchler[30] employing the Hamada-Johnston interaction potential, but in their analysis a rather small contribution of the $l=1$ transfer component was found. Detailed studies of these effects should also be made for inelastic processes with composite projectiles. In particular, calculations for the (^{3}He,^{3}He') excitation did not succeed in predicting the extremely forward angular distribution (see Fig. 7). It was found here that the $l=2$ transfer component arising from the $(\vec{\sigma}\cdot\vec{\sigma})$ type central interaction is too small to fill up the sharp dip of the $l=0$ angular distribution at extremely forward angles, although such an $l=2$ component would reproduce the broad peak observed. A similar discrepancy was found in the (^{3}He,^{3}He') process leading to the ^{12}C 15.11-MeV ($1^+, T=1$) state, and also for the analogous (^{3}He,t) process leading to the ^{12}N(g.s.) ($1^+, T=1$) state.[7] These facts may be showing the importance of one-nucleon pickup and stripping type second-order processes for the (^{3}He,^{3}He') process, which has been found important in the (^{3}He,t) charge exchange processes,[31] and can provide the $l=2$ transfer.

Despite such ambiguities, it may still be worthwhile to compare the strength $V_{10}=2.9$ MeV found in the analysis of (p,p') by Mori[10] for the 1.6-fm Gaussian form nucleon-nucleon interaction with that extracted from the present analyses. The former can be converted to an equivalent strength V_{10}(Y-1.0) = 5.3 MeV of the Yukawa form with 1.0-fm range nucleon-nucleon interaction compared to the present value of 8.28 MeV (see Table II). Such differences indicate the need for more detailed treatments including exchange effects.

The nuclear wave function used here for the excited 1^+ state was taken to be the $(p_{3/2}^{-1}p_{1/2})$ configuration.[21] The single-particle wave functions were calculated by the separation energy method using the Woods-Saxon potential (see Sec. III for details). The γ-transition width of the $M1$ decay to the ground state was calculated using these wave functions to be $\Gamma_{\gamma_0}=0.67$ eV, which should be compared with the observed width[24] 0.35 ± 0.05 eV. Such large transition strengths due to the use of simple jj-shell model wave function were also found[29] in analyses of (p,p') data at 160- and 100-MeV incident energies. About a factor of 10 times larger cross sections were obtained by the calculations using the WKB impulse approximation. Kawai, Terasawa, and Izumo[27] studied spin-flip excitations by the (p,p') process for the sd-shell nuclei where the single-particle picture of $d_{3/2} \rightarrow d_{5/2}$ transition gives about 3 times larger $M1$ decay width than that observed. Reduction of this

overenhanced value was dramatically achieved by the inclusion of configuration mixing (see comments in Ref. 27). This suggests that the nuclear transition matrix element calculated in the present study may be subjected to a similar reduction if a more precise wave function is employed, and then the interaction strengths obtained here could be increased by a factor of 1.4 which turns out, for instance, to be V_{10}(Y-1.0) = 11.7 MeV on the average for the (d,d') at 28 MeV excitation, or 7.42 MeV if a simple correction is done for the exchange effect based on Mori's calculation.

The analysis of the 4.43-MeV (2^+) state excitation in the 28-MeV (d,d') scattering was made employing the simple $p_{3/2} \rightarrow p_{1/2}$ excitation picture. The $E2$ decay width from the 2^+ state to the ground state was calculated using the same wave function used for the (d,d') analysis, with the result $\Gamma_{sp}(E2)$ = 2.08 meV, while the experimental value is $\Gamma_{exp}(E2) = 10.8 \pm 6$ meV.[32] It again yields the reduction factor of 2.3 if we assume the same enhancement due to the collective nature of the 2^+ state wave function. A similar collective enhancement in the inelastic excitation has been discussed by Hinterberger *et al.*[12] in their microscopic analysis of (d,d') at 52 MeV using the Gillet-Vinh Mau shell model wave function.[21] They found that the required interaction strength was reduced by a factor of 1.8 from that obtained by using the simple $p_{3/2} \rightarrow p_{1/2}$ excitation model. All these findings point out the strong effects of the configuration mixing. It is thus quite important to note that microscopic treatments of inelastic excitation provide a very sensitive test of the wave function. It also points out that any microscopic calculation faces such complexities in details, and further efforts must be made to refine the theory in the future.

The investigation of the $^{12}C(\alpha,\alpha')^{12}C$ excitations at 36 MeV was done by Cecil and Peterson.[33] The calculations of differential cross sections to excite 4.43-MeV (2^+) and 9.64-MeV (3^-) states have been done with the microscopic description for the target nucleus but regarding the α projectile as an elementary particle. They also used the Gillet-Vinh Mau wave function. The α-nucleon interaction had the Yukawa form with 1.0-fm range and the strength was found to be 430 MeV. Converting this strength to the nucleon-nucleon interaction strength using $\gamma = 0.329$ fm^{-1} for the Gaussian type α wave function from Ref. 1, we find 64.3 MeV for V_{00}(Y-1.0) which is quite compatible with 51.9 MeV obtained above.

One of the most important aims of the present investigations was to test such a model for the spin-flip excitation process by the $(^6Li, ^6Li')$ inelastic scattering assuming the $^6Li = d + \alpha$ cluster model. As shown in Sec. IV B, a reasonable agreement with the observed data was obtained, at least for the shape of the angular distribution, thus providing a possible justification for the present model. A conclusive result about the strength of the calculated cross section cannot be obtained here because of the ambiguities in the extraction of the basic strength of the (d,d') effective interaction where we had to introduce a radial cutoff parameter. However, it should also be noticed that the strength of 8.73 MeV which is needed for reproducing the observed cross section is rather close to 7.42 MeV where the exchange effects and the configuration mixing of the wave function were simply estimated, though such a simplification should be taken with caution. This strength is also very close to those found by Ball and Cerny in p-shell nuclei.[7]

Other related problems are to be noted: (1) The optical potential of the $^6Li + ^{12}C$ scattering system calculated by the folding method using the cluster model for ^6Li was quite different[34] from those found by the phenomenological parameter search. Particularly, the imaginary part is considerably different. (2) The $^{12}C(\alpha,\alpha')^{12}C$ 12.71 MeV ($1^+, T = 0$) excitation is expected to be a strongly forbidden process because of the spinless α projectile. The experimental measurement has been done by Cecil and Peterson[33] for the 36-MeV incident energy and the peak cross section is about 1 mb/sr at the angle $\theta_{c.m.} = 15^\circ$ which is larger than those of the present (d,d') at 28 MeV (about 0.5 mb at the forward angles, see Fig. 4) and of the $(^6Li, ^6Li')$ excitations (about 0.07 mb).

For the first question, the importance of composite properties of the ^6Li nucleus or the Pauli principle should be remembered, and therefore such a simple folding model for producing the Wigner part of the central potential cannot represent the phenomenological optical potential. Neglect of the decay channels of the weakly bound ^6Li system brings about more difficulties for the imaginary part. However, for the present specific spin-dependent channel, only the deuteron cluster part should play a role and the existence of the α cluster should not disturb such a spin-dependent interaction between the deuteron cluster and target nucleus. The same situation has been found[35] in the calculation of the spin-orbit potential of the $^6Li + ^{12}C$ scattering system by the use of a basically similar picture used here and it was found that the folding model gave successful results.

For the second question, one may remember that this excitation induced by α particles can only proceed through second or higher-order processes. These were investigated by Cecil and Peterson by considering the successive nucleon stripping

and pickup processes and also the successive inelastic excitation processes through the 2^+ and 3^- intermediate states of ^{12}C. A crude estimate may be made for those higher-order contributions to the (^{6}Li, ^{6}Li′) process arising from the α-cluster part. Assuming first that the whole (^{6}Li, ^{6}Li′) cross section arises from the inelastic scattering of the deuteron cluster part, the reduction factor of the free (d,d') cross section due to the deuteron being bound inside the ^{6}Li projectile may be an order of 0.07 mb/0.5 mb $\approx$ 0.1, which is caused mainly from the bound nature of the deuteron inside the ^{6}Li and the stronger suppression of nuclear interior contributions in the (^{6}Li, ^{6}Li′) than those in the (d,d'). The same order of reduction should occur for the α-cluster part, but the square of this reduction factor should be multiplied to the free (α,α') excitation cross section (1 mb at peak), since the possible lowest excitation processes are in the second order. Then a rough estimate for the (α,α') contribution to the (^{6}Li, ^{6}Li′) excitation is about 10 μb. This magnitude should be compared with the 70 μb of the (^{6}Li, ^{6}Li′) peak cross section and one may conclude that the (α,α') contributions are very small.

It is interesting to note that applications of the cluster description of lithium nuclei showed quite successful results in three different cases: the (^{7}Li, ^{6}Li) reaction,[3] the spin-orbit potential of the ^{6}Li + ^{12}C scattering,[35] and the present spin-flip inelastic scattering.

VI. CONCLUDING REMARKS

The excitation mechanisms of (d,d') and (^{6}Li, ^{6}Li′) leading to the ^{12}C 12.71-MeV ($1^+, T=0$) state were studied in the framework of DWBA with microscopic descriptions for both projectile and target systems. For the (^{6}Li, ^{6}Li′) scattering, the α-spectator model was tested assuming the $\alpha+d$ cluster configuration where only the d-cluster part was supposed to contribute to the spin-flip excitation while the α-cluster part acts as a spectator. The form factor for the (^{6}Li, ^{6}Li′) calculation is provided in principle mainly from the analysis of the (d,d') excitation without any other free parameters.

The $(\vec{\sigma}\cdot\vec{\sigma})$ type central interaction was assumed for the present (d,d') calculation. Four different forms of interaction potentials were tested: a Yukawa form with range 1.0–1.2 fm, and a Gaussian form with range 1.16–1.57 fm (see Table I). The results were compared with and fitted to the observed results of (d,d').[5,6] The interaction strength extracted was 8.28 MeV on the average, which is an equivalent nucleon-nucleon interaction strength V_{10}(Y-1.0) of Yukawa form with 1.0-fm range for the $s=1$ and $t=0$ transfer. This value is quite consistent with that obtained from the analysis of (^{3}He, ^{3}He′) (Ref. 7; see Table II).

Because of a momentum mismatch problem due to the present rather low incident energy of 28 MeV for the (d,d') process, the use of a lower radial cutoff (LRC) was necessary in DWBA calculations to reproduce the observed angular distribution. With LRC = 2.3 fm, a reasonable fit of the calculated angular distribution to the data was obtained (see Fig. 3), but the interaction strength was increased to 20.2 MeV. Therefore, it is suggested that a check be made on whether the strength of about 10 MeV will result again from the analysis of high enough incident energy data for the (d,d') scattering without the ambiguity of radial cutoff.

The results from the (d,d') analyses thus obtained were utilized in the (^{6}Li, ^{6}Li′) calculation, and it was found that the present model can reproduce consistently the shape of the angular distribution of the (^{6}Li, ^{6}Li′) experimental data.[19] The magnitudes of the calculated cross section are consistent with the observed result if we use the strength of 8.28 MeV (without cutoff case) and about 5 times larger for 20.2 MeV (with the cutoff case).

Effects of more complex interactions were discussed in general including the effects of the tensor force, exchange processes, and two-step processes. The configuration mixing in the target ^{12}C nucleus seems to be also an important factor to finalize the interaction strength extracted.

The (d,d') excitation leading to the ^{12}C 4.43-MeV (2^+) state was also studied. The result of the calculation was compared with and fitted to the observed data.[5,6] The extracted interaction strength of the Wigner part of the nucleon-nucleon interaction strength was found to be quite consistent with those previously obtained in the (d,d'),[12] (^{3}He, ^{3}He′)[7] (see Table III), and (α,α') (Ref. 32) analyses.

One of the authors (K.-I. K.) appreciates the hospitality accorded to him by T. T. Sugihara and the Cyclotron Institute staff at Texas A & M University.

APPENDIX

The DWBA differential cross section is given using the T matrix defined by Eq. (1)

$$\frac{d\sigma}{d\Omega} = \frac{\mu_a\mu_b}{(2\pi\hbar^2)^2}\frac{k_f}{k_i}\frac{1}{(2J_a+1)(2J_A+1)}\sum_{M_aM_bM_AM_B}|T_{fi}|^2, \tag{A1}$$

where μ_a and μ_b are the reduced masses of projectile and ejectile, respectively. The distorted waves are expanded into partial waves. Then Eq. (A1) may be expressed as follows,[13]

$$\frac{d\sigma}{d\Omega} = \frac{1}{2J_A+1}\frac{1}{4\pi}\frac{1}{E_i E_f}\frac{k_f}{k_i}\sum_{j\mu M_a M_b}(2j+1)^2\left|\sum_{ls}\beta^{lsj}_{\mu M_a M_b}(\theta)\right|^2, \tag{A2}$$

where the reduced reaction amplitude $\beta^{lsj}_{\mu M_a M_b}(\theta)$ is

$$\beta^{lsj}_{\mu M_a M_b}(\theta) = \sum_{l_f j_f l_i j_i}\hat{j}_f\hat{l}_i\hat{l}_f^2(l_f 0 l 0|l_i 0)(l_i 0 J_a M_a|j_i M_a)(l_f m_f J_b M_b|j_f\mu_f)(j_f\mu_f j-\mu|j_i M_a)$$
$$\times\begin{pmatrix} l_f & J_b & j_f \\ l & s & j \\ l_i & J_a & j_i \end{pmatrix}\left(\frac{(l_f-m_f)!}{(l_f+m_f)!}\right)^{1/2} i^{l_i-l_f-l}I^{lsj}_{l_f j_f l_i j_i}P^{m_f}_{l_f}(\theta), \tag{A3}$$

and the overlap integral $I^{lsj}_{l_f j_f l_i j_i}$ is defined by

$$I^{lsj}_{l_f j_f l_i j_i} = \int dr\,\chi_{l_f j_f}(k_f r)f_{lsj}(r)\chi_{l_i j_i}(k_i r). \tag{A4}$$

In Eq. (A4), $\chi_{l_i j_i}$ and $\chi_{l_f j_f}$ are the radial parts of the initial and final distorted partial waves, respectively. The function $f_{lsj}(r)$ is the so-called form factor, which contains details of the nuclear structure of the projectile and target systems as well as the interaction potential, and it is given by using the physical quantities defined in Sec. II,

$$f_{lsj}(r) = \sum_{l_1 l_2 j_1 j_2\alpha_1\alpha_2}S(jJ_A J_B; j_1 j_2\alpha_1\alpha_2)S'(sJ_a J_b; t\,T_a T_b)$$
$$\times\sum_{\tau}(-)^{T_a-\tau_a}(T_a\tau_a T_b-\tau_b|t-\tau)\sum_{\beta_1\beta_2}(-)^{(1/2)-\beta_1}(\tfrac{1}{2}\beta_1\tfrac{1}{2}-\beta_2|t-\tau)D(\alpha\beta t)(-)^{l+s+j}\hat{l}\,\hat{s}^2\hat{J}_a^{-1}\hat{j}_1\hat{j}_2$$
$$\times\begin{pmatrix} j_1 & \frac{1}{2} & l_1 \\ j_2 & \frac{1}{2} & l_2 \\ j & s & l \end{pmatrix} i^{l_1-l_2}\langle l_2||Y_l||l_1\rangle\bar{V}_{st}f_l(r). \tag{A5}$$

In Eq. (A5), $\bar{V}_{st}$ is the strength of the projectile-nucleon interaction, defined by Eq. (6) and $f_l(r)$ is the radial factor defined by Eq. (9c) for the (d,d') process. The nuclear transition matrix element $K_{M_B M_b, M_A M_a}$ given by Eq. (4a) is expressed using the form factor defined by Eq. (A5) as follows:

$$K_{M_B M_b, M_A M_a}(\vec{r}) = \sum_{jls}(-)^{J_A-M_A}(J_A M_A J_B - M_B|j-\mu)(-)^{J_a-M_a}(J_a M_a J_b - M_b|s-\sigma)$$
$$\times(-)^{s-\sigma}(lms-\sigma|j\mu)(-)^{l+j}\hat{J}_a\hat{s}^{-1}\hat{l}^{-1}f_{lsj}(r)i^l Y^*_{lm}(\hat{r}). \tag{A6}$$

The expressions shown above can also be used for the present α-spectator model in the (^{6}Li,^{6}Li′) spin-flip excitation process with the following two changes: The radial coordinate r is replaced by R, and the radial factor $f_l(r)$ is replaced by $f_l(R)$ given by Eq. (12b). The radial parts of distorted waves appearing in Eq. (A4) are, of course, those of ^{6}Li scattering.

---

*Supported in part by the National Science Foundation.

†On leave of absence from Department of Physics, University of Tokyo.

[1]V. A. Madsen, Nucl. Phys. 80, 177 (1966).

[2]P. J. Moffa, J. P. Vary, C. B. Dover, C. W. Towsley, R. G. Hanus, and K. Nagatani, Phys. Rev. Lett. 35, 992 (1975).

[3]K.-I. Kubo, H. H. Duhm, and N. Ueta, Phys. Lett. 45B, 299 (1973).

[4]The basic idea of systematic analyses for these processes was previously proposed by P. A. Assimakopoulas, G. Andritsopoulos, N. H. Gangas, and K. Nagatani, Bull. Am. Phys. Soc. 19, 431 (1974).

[5]W. J. Braithwaite (private communication). Thanks are due him for making the data available prior to publication.

[6]J. M. Lind, G. T. Garvey, and R. E. Tribble, Nucl. Phys. A 276, 25 (1977).

[7]G. C. Ball and J. Cerny, Phys. Rev. 177, 1466 (1969); the interaction strength V_{10}(Y-1.0) extracted in this

work was obtained by using a different set of distorting potential parameters (AVERAGE SET). Also a correction factor of 0.87 which was multiplied to the strength obtained normalizing the calculated cross section to the experimental data.

[8]E. L. Petersen, I. Šlaus, J. W. Verba, R. F. Carlson, and J. R. Richardson, Nucl. Phys. A102, 145 (1967).

[9]G. R. Satchler, Nucl. Phys. A100, 497 (1967).

[10]A. Mori, Nuovo Cimento Lett. 1, 703 (1971).

[11]W. G. Love and L. J. Parish, Nucl. Phys. A157, 625 (1970).

[12]F. Hinterberger, G. Mairle, U. Schmidt-Rohr, G. J. Wagner, and P. Turek, Nucl. Phys. A115, 570 (1968).

[13]G. R. Satchler, Nucl. Phys. 55, 1 (1964).

[14]J. J. Wesolowski, E. H. Schwarcz, P. G. Ross, and C. A. Ludemann, Phys. Rev. 169, 878 (1968).

[15]K. Wildermuth and W. McClure, *Springer Tracts in Modern Physics* (Springer, Berlin, 1966), Vol. 41.

[16]M. Moshinsky, Nucl. Phys. 13, 104 (1959).

[17]A. R. Edmonds, *Angular Momentum in Quantum Mechanics* (Princeton U.P., Princeton, 1957).

[18]G. Perrin, Nguyen Van Sen, J. Arvieux, A. Fiore, J. L. Durand, R. Darves-Blanc, J. C. Gondrand, F. Merchez, and C. Perrin, Nucl. Phys. A193, 215 (1972).

[19]P. K. Bindal, K. Nagatani, M. J. Schneider, and P. D. Bond, Phys. Rev. C 9, 2154 (1974).

[20]K.-I. Kubo and M. Hirata, Nucl. Phys. 187, 186 (1972).

[21]V. Gillet and N. Vinh Mau, Nucl. Phys. 54, 321 (1964).

[22]F. D. Reisman, P. I. Connors, and J. B. Marion, Nucl. Phys. A153, 244 (1970).

[23]W. J. Braithwaite, J. E. Bussoletti, F. E. Cecil, and G. T. Garvey, Phys. Rev. Lett. 29, 376 (1972).

[24]F. E. Cecil, L. W. Fagg, W. L. Bendel, and E. C. Jones, Jr., Phys. Rev. C 9, 798 (1974).

[25]N. Austern, *Direct Nuclear Reaction Theories* (Wiley, New York, 1970).

[26]F. G. Perey and B. Buck, Nucl. Phys. 32, 353 (1962).

[27]M. Kawai, T. Terasawa, and K. Izumo, Nucl. Phys. 59, 289 (1964); the configuration mixing reduces the mixing amplitude of such simple ph-coupling component, and there happens a destructive interference of the $d_{3/2} \rightarrow d_{5/2}$ decay and $d_{5/2} \rightarrow d_{3/2}$ decay.

[28]D. Hasselgren, P. U. Renberg, O. Sundberg, and G. Tibell, Nucl. Phys. 69, 81 (1965).

[29]H. K. Lee and H. McManus, Phys. Rev. 161, 1087 (1967); Y. S. Horowitz and R. E. Bell, Can. J. Phys. 48, 201 (1970).

[30]W. G. Love and G. R. Satchler, Nucl. Phys. A159, 1 (1970).

[31]M. Toyama, Phys. Lett. 38B, 147 (1972); K.-I. Kubo, Nucl. Phys. A246, 246 (1975), and references therein.

[32]F. Ajzenberg-Selove, Nucl. Phys. A248, 1 (1975).

[33]F. E. Cecil and R. J. Peterson, Phys. Lett. 56B, 335 (1975).

[34]J. W. Watson, Nucl. Phys. A198, 129 (1972).

[35]K.-I. Kubo and H. Amakawa, in *Proceedings of the Fourth International Symposium on Polarization Phenomena in Nuclear Reactions, Zurich, 1975*, edited by W. Grüebler and V. König (Birkhäusen, Basel, 1976), p. 829; W. Weiss, P. Egelhof, K. D. Hildenbrand, D. Kassen, M. Makowska-Rzeszutko, D. Fick, H. Ebinghaus, E. Steffens, A. Amakawa, and K.-I. Kubo, Phys. Lett. 61B, 237 (1976).